J. Physiol. (1979), **289**, *pp.* 375–388
With 5 text-figures
Printed in Great Britain

INITIATION AND SPREAD OF ACTION POTENTIALS IN GRANULE CELLS MAINTAINED *IN VITRO* IN SLICES OF GUINEA-PIG HIPPOCAMPUS

BY J. G. R. JEFFERYS*

From the Physiology Department, University College London, Gower Street, London WC1E 6BT

(*Received 6 June 1978*)

SUMMARY

1. Laminar field potentials due to the synchronous activation of granule cells were studied in slices of guinea-pig hippocampus maintained *in vitro*.

2. Extracellular recordings confirmed that stimulation of afferent laminae in the molecular layer caused excitatory synaptic current to enter the granule cell dendrites. If large enough this current initiated action potentials at, or near to, the somata 100–200 μm away.

3. After a population spike had been initiated via excitatory synapses or via antidromic invasion, the location of inward membrane current (sink) appeared to move from the cell body layer into the dendrites at a velocity of 0·08–0·12 m/sec, for a distance of up to 250 μm.

4. The sink movement into the dendrites was blocked by tetrodotoxin and not by agents that blocked synaptic activation. Together with other observations these results led to the conclusion that granule cell dendrites were invaded by action potentials from the cell body region. There was no evidence of dendritic action potentials preceding the cell body spike initiated by synaptic inputs. Possible functions of this dendritic invasion are discussed.

INTRODUCTION

The response of central neurones to incoming impulses depends on the properties of their dendrites. An important factor may be whether or not the dendrites support action potentials. The work presented here investigates the site of initiation and the subsequent development of action potentials in hippocampal granule cells. These neurones are small (10–12 μm soma diameter), and it would be difficult to record intracellularly from their dendrites. Extracellular field potentials can nevertheless provide evidence on the location of current flows across the dendritic membranes. The tight layering (laminar organization) of the granule cell bodies and of the afferent tracts to their dendrites simplifies the interpretation of the field potentials. The basic features of these evoked potentials have already been described both *in vivo* and

* Present address: Neurological Science Dept, Royal Free Hospital Medical School, Pond St, London NW3 2QG.

0022-3751/79/3030-0511 $01.50

in vitro (Andersen, Holmqvist & Voorhoeve, 1966; Andersen, Bliss & Skrede, 1971; Lømo, 1971; Bliss & Richards, 1971; Skrede & Westgaard, 1971).

The interpretation of field potentials in terms of events at the neurone has in some circumstances proved controversial, especially when dendritic spikes might have been involved. An example of this type of argument concerned the Purkinje cell of the alligator cerebellum (Llinás, Nicholson, Freeman & Hillman, 1968; Calvin & Hellerstein, 1969; see also Discussion of this paper). In such cases conclusions derived from a thorough consideration of the field potentials (e.g. Nicholson & Llinás, 1971) may be strengthened by independent kinds of evidence. In the alligator example it was possible to obtain intracellular recordings from the cells and their dendrites (Llinás & Nicholson, 1971). In the present study it has been possible to test some of the conclusions from field potential analyses by manipulating the environment of *in vitro* brain slices from the hippocampus.

METHODS

Albino guinea-pigs, 300–650 g in weight, were killed by cervical dislocation. The brain was removed quickly and slices were taken from either the ventral surface of the dentate area, exposed by blunt dissection (longitudinal slices; Bliss & Richards, 1971; Yamamoto & Kawai, 1967), or from a surface cut perpendicular to the long axis of the hippocampus (transverse slices; Skrede & Westgaard, 1971). Slices were cut freehand with a Gillette Valet blade, and their thickness was controlled by the use of a simple recessed glass cutting guide (300–500 μm deep) placed on the tissue surface. Slices were placed in oxygenated artificial c.s.f. within 5 min of the animals' death and experiments started about 30 min later.

The slice bath was designed to hold the slice, immersed in the circulating artificial c.s.f., between a nylon net and a set of parallel hairs, each supported on nylon rings. These rings had a push fit in the moulded silicone rubber walls of the slice chamber. The bathing medium was circulated at 1·5 ml./min by a peristaltic pump between the slice chamber (3 ml.) and a reservoir (22 ml.). Two reservoirs were included in the bath to allow for changes of solution, the outlet from each to the slice chamber being controlled by a screw tap. Temperature was controlled by water, from a thermostatically controlled water-bath, circulated through a jacket which contained the reservoirs and slice chamber. The artificial c.s.f. normally had the following composition (mM): NaCl, 135; $NaHCO_3$, 16; KCl, 3; $CaCl_2$, 1·5; NaH_2PO_4, 1·25; $MgCl_2$, 1·0; glucose, 10; equilibrated with a mixture of 95 % O_2 and 5 % CO_2 before use and while in the reservoirs.

Recording and stimulating methods were conventional. Micropipettes for recording were filled with 3 M-NaCl solution and had resistances in the range 1–4 MΩ. Electrodes for stimulation were made from 10 μm diameter platinum wire insulated to 10–20 μm of the tip. Evoked potentials were recorded from an oscilloscope on 35 mm film or sometimes on FM magnetic tape for subsequent analysis on a digital computer. Filters were set to 8 Hz (high pass) and 2·5 kHz (low pass).

Currents crossing cell membranes in the granule cell layers were inferred from the second spatial derivative of potentials recorded at sites across the laminae, at particular instants after stimuli. Derivatives were estimated from the differences between potentials at twice the 25 μm spacing of the recording sites. This reduced the effect of errors in the positioning of electrodes and was numerically equivalent to repeating twice a procedure of averaging adjacent points. In order to avoid making uncertain assumptions, the data obtained from spatial derivatives of extracellular voltage are calibrated in units of V/m and V/m^2. Approximately equivalent extracellular current densities and current sink densities can be obtained by multiplying these figures by a value for the tissue impedance, *ca.* 70–500 Ω.cm (Ranck, 1963; Freeman & Stone, 1969; Yedlin, Kwan, Murphy, Nguyen-Huu & Wong, 1974; Nicholson & Freeman, 1975). The precisely appropriate impedance measure is controversial, however, and since the main interest of the data concerns comparisons of the relative values of current sink densities, the units are left in those which most directly relate to the original data.

RESULTS

Sequence of events during granule cell responses. The responses illustrated in Fig. 1 were due to stimulation of an afferent path. Evoked potentials were recorded at sites evenly spaced along a track across the granule cell layers (Fig. 1*A*, *C*). Potential

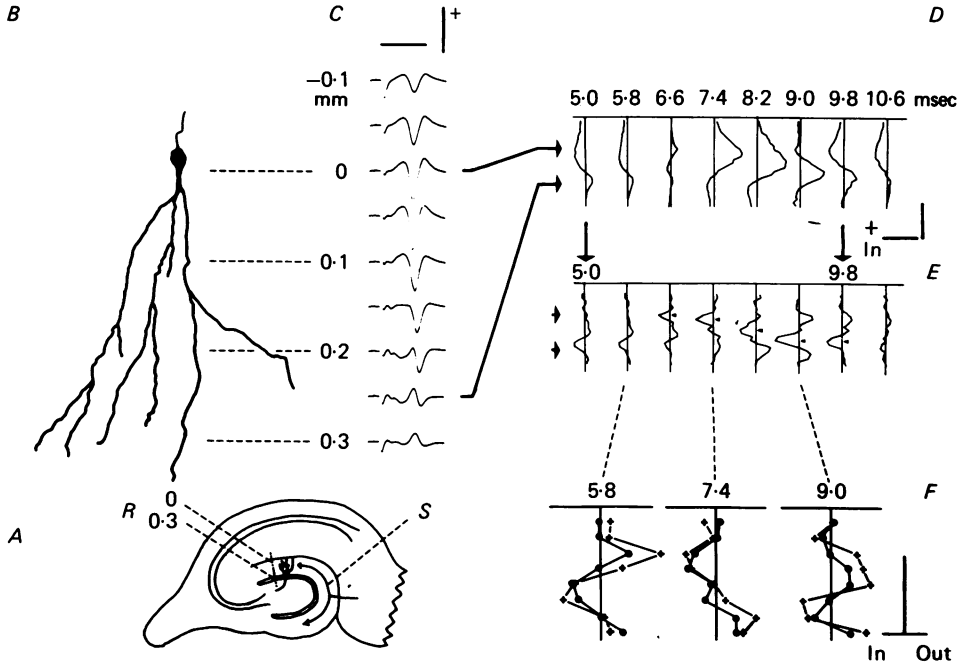

Fig. 1. Granule cell responses to stimulation of afferent laminae. Potentials were recorded on a track perpendicular to the cell layers in a transverse slice (*A*). The potentials illustrated in *C* are lined up with a *camera lucida* drawing of a granule cell (*B*), which was scaled (× 1·25) to bring into register the hippocampal fissures and the cell body layers of the two parts. Potential profiles (*D*) were drawn from measurements made at each of eight times after the stimulus. The second spatial derivatives of these profiles, approximated by a numerical method, provide an indication of membrane current (*E*). The sites of maximum inward membrane current after initiation of the population spike have been marked ▲. Corresponding recording sites in *C*, *D* and *E* are indicated by arrows. Profiles from another experiment (on a longitudinal slice) reveal the effect, on estimates of membrane current from a single track (●), of corrections for currents parallel to the cell layers (+). Dashed lines between *E* and *F* indicate similar phases in the two responses, which fortuitously had similar time courses (calibrations: potentials, *C* and *D*, 0·5 mV; second derivatives, or 'membrane current', *E* and *F*, 0·15 V/mm²; time, *C*, 10 msec; distance, *D*, *E* and *F* 250 μm).

profiles along this track have been plotted for each of eight times after the stimulus (Fig. 1*D*). The second spatial derivative of these potential profiles can be used to estimate membrane current (Humphrey, 1968; Freeman & Stone, 1969). Tissue resistance has not been estimated here, so the second spatial derivative of potential and the membrane current are at best proportional (if the resistance is uniform across the cell laminae and during the response), and possibly only qualitatively related. However, for convenience the term 'membrane current' will be used in the

description of second derivatives. Second derivative profiles of the post-synaptic response are illustrated in Fig. 1*E*.

Inward membrane current (or a sink of extracellular current) was recorded 3·4–7·0 msec after the stimulus to the afferent laminae, in the middle molecular layer,

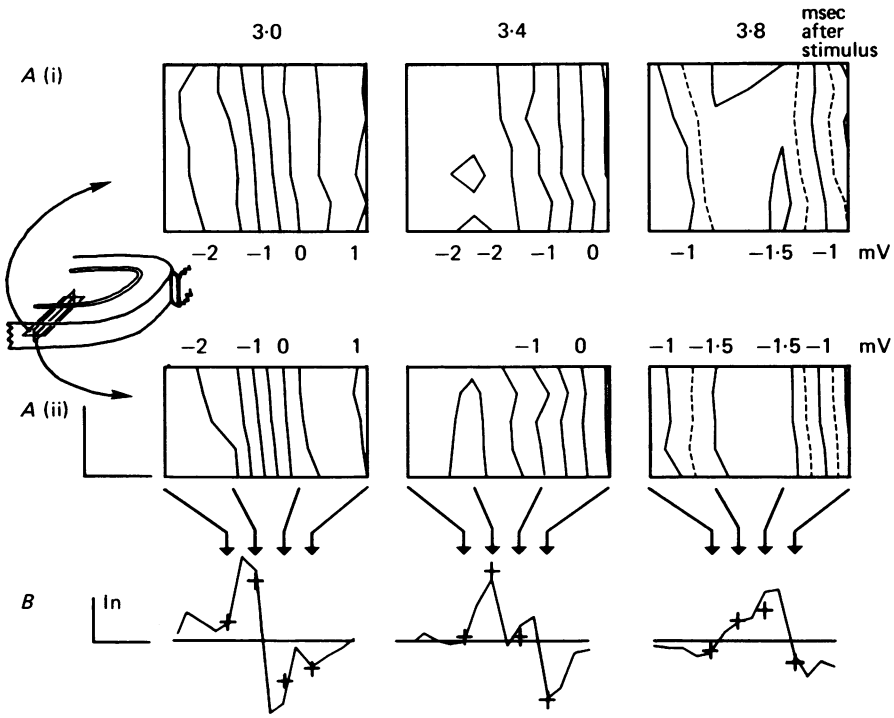

Fig. 2. Isopotential contours in planes perpendicular to the granule cell layer during antidromic activation. Three orthogonal recording axes were carefully aligned with the plane of the granule cell body layer in a transverse slice (kept at 34 °C). *A*, isopotential contours have been plotted for three times after the stimulus, using linear interpolation between potentials measured from the regularly spaced recording sites. The vertical axes in *A* represent the direction of the cell body layer. *B*, superimposed on the second spatial derivatives of potential profiles from the intersection of the recording planes are values corrected for the small potential gradients perpendicular to this intersection (+) (calibrations: *A*, 50 μm in both axes, contours at 0·5 mV; *B*, 0·5 V/mm^2 inward current up, 100 μm).

150–200 μm from the cell body layer (Fig. 1*E*). This corresponds to the extracellular e.p.s.p. or synaptic wave (Lømo, 1971). At sites where this inward synaptic current could be detected, it was preceded by a small biphasic potential (Fig. 1*C*, 0·2 mm), which could be attributed to the presynaptic fibre volley as it was resistant to 12 mM-$MgCl_2$ and to 3 mM-$MnCl_2$, each in the absence of Ca ions. The subsequent post-synaptic components were abolished by these treatments (Fig. 3*A*). Inward current at the cell body layer, recorded 6·6 msec after the stimulus in the present example, corresponds to a population spike (Andersen *et al.* 1971). Although the spike was initiated in the granular layer, it is not possible to tell whether action potentials were triggered at the somata or at neighbouring parts of the cells. In the later profiles of Fig. 1*E* (8·2–9·8 msec after the stimulus) the site of inward membrane

current, which is marked by small triangles in the Figure, appeared to move into the dendritic layers at a velocity of 0·1 m/sec and for a distance of 175–200 μm. The sink drew current from sources (regions of outward membrane current) in the more distal dendrites and also in the region of the cell bodies. The location of maximum inward current at each instant in the response (Fig. 1 *E*) was close to the most negative site in the corresponding potential profile (Fig. 1 *D*).

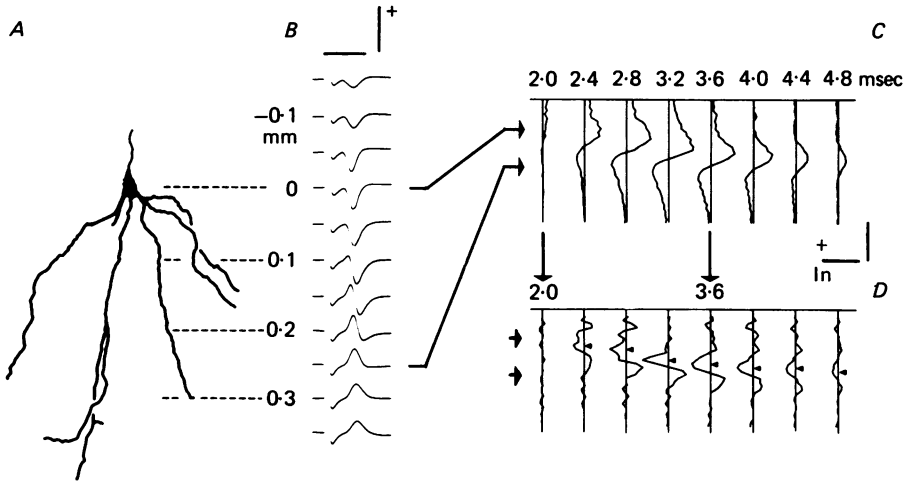

Fig. 3. Granule cell responses to stimulation of their axons. Refer to Fig. 1, parts *B* to *E* for explanation of parts *A* to *D*. Results obtained from a single track in a longitudinal slice kept at 38 °C (calibrations: *B*, 1 mV, 5 msec; *C*, 1 mV, 250 μm; *D*, 0·3 V/mm², 250 μm).

In the present work membrane currents are inferred from the second spatial derivative of potential profiles across the cell layers. Spurious membrane currents could be inferred if the extracellular currents were not strictly perpendicular to the cell laminae. This was not important under the present recording conditions. An example is illustrated (Fig. 1 *F*) where potentials have been recorded at 50 μm intervals along a line perpendicular to the cell layer and also on four other parallel tracks, 50 μm away, so that each site on the central track (except at its ends) was 50 μm from a recording site in each of three orthogonal axes. The second spatial derivative of voltage has been estimated along each of the axes about the points in the central track. Profiles of the second derivative along the central track alone (open circles, Fig. 1 *F*) are compared with those corrected for the effects of currents perpendicular to this track (crosses, Fig. 1 *F*). These corrections did have some effect on the size of the second derivatives, but did not alter the over-all pattern of events. Thus the single track and corrected profiles both show inward synaptic current at 5·8 msec, the cell body layer sink (population spike) at 7·4 msec and the late dendritic sink at 9·0 msec.

The degree of lamination of the field potentials is illustrated by the isopotential contours obtained from recordings in two orthogonal planes perpendicular to the cell layers (Fig. 2). The contours are orientated vertically, which corresponds to axes parallel to the cell layers in the slice. Thus the maximum extracellular current,

which is perpendicular to the isopotential contours, was at right angles to the cell layers. Second derivative profiles have been constructed for the track at the intersection of the two recording planes (Fig. 2*B*) and corrections applied for the effects of currents perpendicular to this track (crosses). These corrections are small. That they are smaller than those shown in Fig. 1*F* could be due to the larger potentials

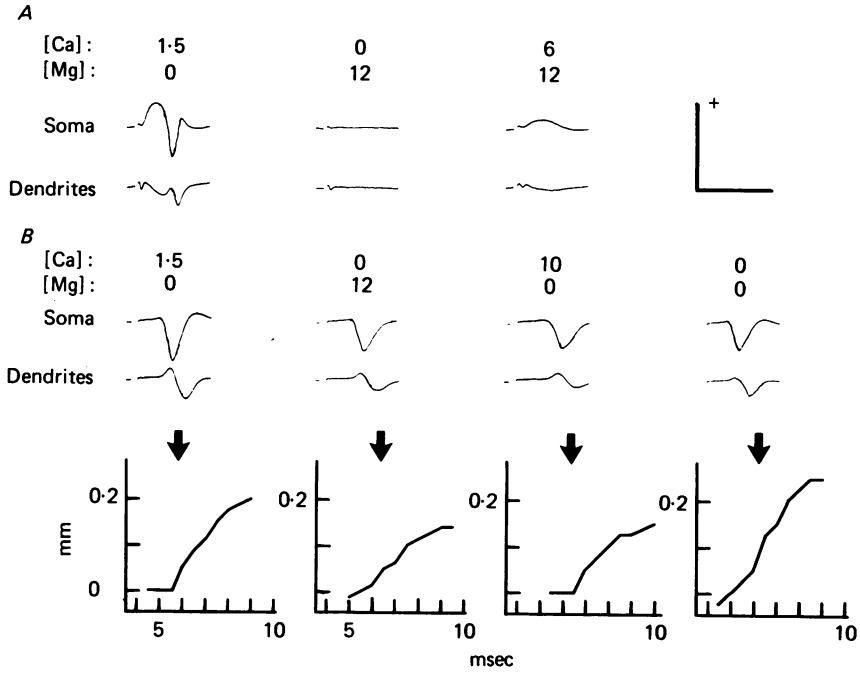

Fig. 4. Effect of Ca and Mg ions on granule cell responses. Post-synaptic (*A*) and antidromic (*B*) responses were recorded from a longitudinal slice, which was immersed in bathing solutions containing various concentrations of Ca and Mg ions (shown in mM at the head of each set of responses). The responses illustrated under each condition were recorded from the cell body layer (upper trace) and from a point 150 μm away in the dendritic region (lower trace). In part *B* full depth profiles have been used to locate the inward current with respect to the cell body layer. This location has been plotted against time after the stimulus for each of the treatments illustrated (calibrations: *A*, 2 mV, 20 msec; *B*, 2 mV, 10 msec; slice kept at 28 °C).

recorded for Fig. 2, or to the faster sweep speed used, or to some inherent difference in the stability of post-synaptic and antidromic responses.

The second derivative profiles of the antidromic response shown in Fig. 2 reveal that a region of inward membrane current moved from the cell body layer into the dendritic region. Antidromic responses, recorded across the cell layers of another slice, show the sequence of events in more detail (Fig. 3). The potential and the second derivative profiles of Fig. 3*C* and *D* are plotted at 0·4 msec intervals. The first event to be detected was due to inward membrane current at the cell body layer, 2·4 msec after the stimulus. As was the case for the population spike evoked by synaptic current (Fig. 1), the site of inward current (triangles, Fig. 3*D*) moved into the dendritic layers at a velocity of 0·1 m/sec and for a distance of 150–200 μm. This sink movement has been detected whenever suitable recordings have been taken

from slices of the dentate area. So far this exceeds 100 repetitions in thirty different slices. The velocity of the movement was in the range 0·08–0·12 m/sec and its distance was between 100 and 250 μm for the standard artificial c.s.f. at 30–38 °C.

Mechanism of the sink movement into the dendritic layers. Antidromic activation of the granule cells has been used to test whether the sink movement depended on the activity of chemical synapses. Solutions containing no calcium and more than 6 mM-Mg or 3 mM-Mn abolished the synaptic response of the granule cells, but not the presynaptic fibre volley. This effect was reversible and could be partially countered by increasing the concentration of Ca to 6 mM (Fig. 4*A*). These treatments did not block the antidromic population spike, nor the movement of the associated sink from the soma layer into the dendrites (Fig. 4*B*). The extent and speed of the sink movement were reduced by the high concentration of Mg used in this experiment (12 mM); but a high concentration of Ca (10 mM), in the absence of Mg, applied to the same slice had a similar effect. In the absence of divalent cations the sink movement was similar to that in the standard artificial c.s.f. In some slices this treatment caused four or five afterdischarges to follow the initial population spike.

The possibility of the sink movement being caused by a dendritic action potential was strengthened by the observations that the sink movement was reversibly slowed (i) by reductions in temperature and (ii) by replacement of some of the extracellular sodium by choline. The conduction velocity became more sensitive to temperature as this was lowered. Thus 10 °C drops from 38, 33 and 28 °C reduced the velocity by factors of 0·86, 0·69 and 0·63 respectively. Replacing the Na of the normal artificial c.s.f. (152 mM) by 60 mM-Na with 92 mM-choline reduced the velocity to 75% and 40 mM-Na with 112 mM-choline caused a reduction to 25% of normal.

Tetrodotoxin (TTX) is known to block specifically the Na channels involved in the generation of action potentials in most axons. To test whether the dendritic invasion was sensitive to TTX it was necessary to apply the toxin to the dendrites without abolishing the population spike. This was achieved, transiently, by allowing TTX to diffuse across the molecular layer from the ependymal surface while monitoring antidromic invasion of the cells. In the longitudinal slice it was possible to apply the toxin in the solution bathing the lower (ependymal) surface of slices held under moist, warm gas (Fig. 5). There was not enough time to record full depth profiles while the TTX diffused across the slice, so two recording electrodes were used to monitor the potential difference between the cell body and mid-dendritic layers. This potential difference reverses as the current sink moves from the cell body region into the dendrites. This is evident in the profiles of Fig. 3, where 2·8 msec after the stimulus the cell body layer was more negative than a site 150 μm away in the dendrites, while 1·2 or 1·6 msec later in the response, when the sink had moved into the dendrites, the potential difference had reversed.

At the start of the experiment illustrated in Fig. 5 TTX was added (at time 0 sec) to the bath reservoir, to give a final concentration of 1 μM in the circulating solution. The late dendrite-negative component (downward deflexion on the potential difference 'sweeps', Fig. 5*B*, or measured at 9 msec and plotted as triangles in part *C*) decreased in size 60 sec after the toxin was added, and had disappeared by 400 sec. The early soma-negative component (upward deflexion in Fig. 5*B* and, measured at 4·5 msec, plotted as circles in *C*) did not diminish until 250 sec into the experiment

and persisted up to 750 sec. Thus the late component, which is associated with the dendritic sink, was affected by the TTX sooner than the earlier component which is associated with the initial current sink at the soma region. This sequence of events, but not this time course, has been recorded in all eight experiments using local application by pipette to transverse slices and three using bulk application to longitudinal slices.

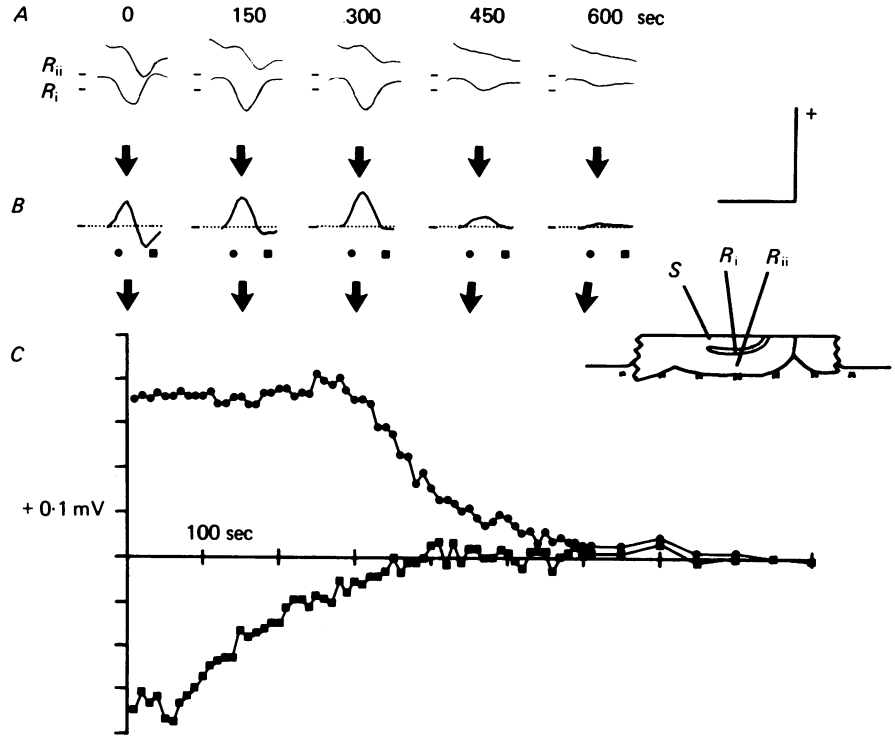

Fig. 5. Action of tetrodotoxin (TTX) on the current sink movement in granule cells. Antidromic granule cell responses were recorded from the cell body layer (R_i) and a point 200 μm away in the dendritic layers (R_{ii}) of a longitudinal slice, which was held at the surface of the bathing solution. At time 0 sec TTX was added to the bathing solution (to a final concentration of 1 μM), and subsequently diffused across the slice from its lower, ependymal surface. *A*, responses are illustrated, recorded at intervals of 150 sec during the experiment. The potential difference between the pairs of responses is plotted below each pair (*B*). *C*, potential differences early (●, 4·5 msec) and late (■, 9·0 msec) in each response during the experiment (every 10 sec) are plotted against time after the addition of TTX. Parts *B* and *C* have been corrected for the stimulus artifact left after TTX had abolished the responses. In these parts an upward deflexion represents soma negativity (calibrations: *A* and *B*, 2·0 mV, 10 msec; base lines retouched in *A*; temperature was 28 °C, which may explain the longer duration of these responses compared with those of Fig. 3).

DISCUSSION

Experiments presented here confirm aspects of previous work on the activation of dentate granule cells *in vivo* (Lømo, 1971) and in slices (Yamamoto & Kawai, 1967; Bliss & Richards, 1971; Skrede & Westgaard, 1971), and explore in more detail the population spike and the events responsible for it. Although the basic pattern of

events is similar, responses from slices do differ from those from the intact animal in some respects. A particularly useful difference is that recordings from slices were very stable and did not show the pronounced variability in measurements of the population spike that is often seen *in vivo* (Lømo, 1971).

Sequence of events during granule cell responses. The pattern of membrane currents in the cell layers was inferred from a succession of depth profiles during the responses (Figs. 1, 3). These results show that the population spike corresponds to an influx of current at the cell body layer. When it was caused by stimuli to afferent fibres, the population spike was preceded by inward current at the afferent lamina (where the putative presynaptic fibre potential could be recorded) and not at layers between the active afferents and the cell bodies (Fig. 1). Thus it is likely that synaptic potentials in the dendrites initiated action potentials at, or near to, the somata by passive spread of current. However, following the population spike, the location of inward membrane current moved up to 250 μm into the dendritic layer, with a velocity of 0·08–0·12 m/sec. This movement was recorded whether the population spike had been initiated by the stimulation of afferents or of granule cell axons.

These conclusions rest on a laminar field potential analysis. The slice preparation (particularly the transverse slice) made easy the orientation of recording profiles with respect to the cell layers. It was possible to compare the potential gradients perpendicular to, with those parallel to, the laminae. Typically the gradients parallel were less than one tenth those perpendicular to the layers, and corrections for them had no consistent effect on estimates of membrane current (Figs. 1*F*, 2). Where corrections have been applied they did not alter the location and timing of the synaptic and the population spike currents and the subsequent movement of a current sink into the dendritic region. Thus these features are not an artifact of the field potential analysis.

Mechanism of the sink movement into the dendritic layer. The experiments described below have been designed to establish the cause of the sink movement into the dendritic, or molecular, layer. In other neural systems, extracellular evoked potentials have been used to infer the existence of propagating dendritic spikes (Fatt, 1957*a*, *b*, cat spinal motoneurone; Llinás *et al.* 1968, alligator Purkinje cell). This argument has proved controversial (Nelson, Frank & Rall, 1960; Calvin & Hellerstein, 1969). In both these examples evidence for dendritic spikes has also been obtained using recordings from within the dendrites of the neurones (Terzuolo & Araki, 1961; Llinás & Nicholson, 1971). This approach might be possible for the rather smaller dentate granule cells, but has not been attempted here. Other evidence is presented which supports the hypothesis that propagating dendritic action potentials are involved.

One possible explanation of the late dendritic sink (described above) is that it was caused by synaptic activity due to recurrent collaterals of the granule cell axons. Either an excitatory input to the dendrites or an inhibitory input to the soma could cause an influx of current to the dendrites. The latter is unlikely as it would not produce the current source recorded close to the tips of the dendrites (Fig. 1*E* at 9·0 msec; Fig. 2*D* at 4·0 msec). It is simple to block chemical synapses *in vitro*. Electrical contacts such as gap junctions might not be affected by such treatments, however, there is no evidence yet for their presence in the dentate molecular layer. Ca-free solutions containing 12 mM-Mg (or 3 mM-Mn) reversibly blocked the post-synaptic granule cell response (and not the afferent fibre volley), while antidromic

activation and the subsequent sink movement persisted. The speed and extent of the sink movement were reduced in the solutions containing elevated Mg, but, as solutions with high Ca levels had a similar effect, this resembles the reduction in excitability seen in axons under similar conditions (Frankenhaeuser & Hodgkin, 1957).

A sufficiently large recurrent projection of granule cell axons across the molecular layer might be a candidate to explain the late dendritic sink. However, it would be surprising if action potentials in such axons could generate currents as large as those from the densely packed granule cells. Inspection of second derivative profiles in the hilus, preceding the antidromic, or following the post-synaptic, population spike (e.g. Fig. 3*D*, 2·0 msec; Fig. 1*E*, 7·4 msec) reveals no evidence of currents in the sub-granular zone, where the mossy fibres and their recurrent collaterals to the basket cells would be active.

Two important alternative hypotheses remain to be tested: that the sink movement was due to an invasion of the dendrites by action potentials or to a mechanism not requiring dendritic spikes. An example of the latter may be called the active re-polarization model (Nelson *et al.* 1960; Terzuolo & Araki, 1961; Nelson & Frank, 1964). In a neurone with inexcitable dendrites, an action potential at the soma would depolarize a progressively larger part of the dendritic tree with time. The sodium influx of the classical action potential is followed by a potassium efflux, which tends to repolarize the membrane more rapidly than would be the case otherwise. This zone of repolarization would also tend to expand into the dendritic tree, resulting in a band of depolarization moving into the dendrites from the soma, and this may be recorded extracellularly as a moving sink.

The sink movement described here does have some properties in common with action potentials in peripheral nerve. For instance its velocity is reduced by replacing some of the extracellular sodium ions with choline (Katz, 1947). Nerve action potentials and the sink movement both speed up as the temperature is increased within a physiological range, though the effect is more marked in mammalian C fibres than in granule cell dendrites. Increases of 10 °C from 18 °C and from 27 or 28 °C increased the velocity of the C fibres by 2·1 and 1·5 times (Paintal, 1973) and of the dendritic sink by 1·6 and 1·3 times.

A more direct approach was designed to test whether the late dendritic sink was sensitive to TTX, which specifically blocks the Na channels involved in most action potentials. In early experiments on transverse slices TTX was applied from micro-pipettes (Jefferys, 1976). It is conceivable that this focal application could have resulted in an increased current flow parallel to the cell layers, so disturbing the laminar potentials and possibly producing spurious changes in the responses. In the experiment described here (Fig. 5) the toxin was applied in the solution bathing the lower, ependymal surface of longitudinal slices, so that the TTX should have been distributed more evenly along the laminae as it diffused through the slice. In both types of experiment the late dendritic sink was blocked tens of seconds before the cell body layer sink. It seems reasonable to conclude that the sink movement was due to an invasion of the dendrites by action potentials which were similar to those found in most axons.

It could be argued that the dendritic invasion is a peculiarity of the slice. However,

similar evoked potentials have been described in the anaesthetized rabbit. Andersen *et al.* (1966) reported a negative peak which became progressively later as they withdrew a recording electrode from the cell body layer through the molecular layer, past the dendrites. They suggested this peak could have been due to a dendritic invasion, though without further analysis there might also be other interpretations. The present work was directed to the testing of such possibilities (see above). Andersen *et al.* (1966) estimated the velocity of the dendritic invasion to be 0·5 m/sec from the latencies of two of their recordings. This is faster than the 0·1 m/sec velocity of the sink movement found in the present study. There are many factors that might contribute to this discrepancy.

Unidirectional conduction of dendritic spikes. The present work provided evidence that an action potential at the soma of a hippocampal granule cell could invade the dendrites, and that excitatory synapses on the dendrites initiated spikes at a trigger zone close to the cell body. This situation resembles that reported for the spinal motoneurone (Fatt, 1957*a*, *b*), and differs from those for the hippocampal pyramidal cell (Spencer & Kandel, 1961; Schwartzkroin & Slawsky, 1977) and for the cerebellar Purkinje cells of alligators and pigeons (Nicholson & Llinás, 1971; Llinás & Hess, 1976) where dendritic action potentials preceded initiation of the soma spike. In at least some cases dendritic spikes which could be initiated directly by synaptic activity were not sensitive to TTX, and probably involved an influx of Ca ions (Llinás & Hess, 1976; Schwartzkroin & Slawsky, 1977). Thus it seems that there are two quite distinct types of dendritic spike, which could have different roles in the functioning of neurones.

If the granule cell dendrites can support action potentials, why were no dendritic spikes detected before the synaptic current initiated a soma population spike? It is possible that synaptic current did trigger dendritic spikes directly but that they were not detected by the field potential analysis. This could have happened if such spikes occurred at a few sites with poor synchrony, or failed to develop fully because of shunting due to widespread synaptic activity, or failed to propagate toward the soma. Evidence against at least some of these possibilities comes from the absence of fast prepotentials from intracellular recordings of granule cells (Deadwyler, Dudek, Cotman & Lynch, 1975; Dudek, Deadwyler, Cotman & Lynch, 1976). It was the presence of fast prepotentials that led Spencer & Kandel (1961) to postulate dendritic spikes in CA1 pyramidal cells. Failure of spike propagation toward the soma could have happened at branch points, where the safety factor probably was low (and could have been lower than for conduction from the soma). Inspection of ten cells from Golgi-Cox preparations of guinea-pig hippocampus suggests this was not responsible for unidirectional conduction, as about one third of dendrites did not branch in the inner third of the molecular layer, and many more extended much of the way across. This region corresponds to that between the cell body layer and the afferent laminae activated in the present study. *Camera lucida* drawings of two of these cells are shown in Figs. 1*B* and 3*A*.

Perhaps the most likely explanation of unidirectional propagation of spikes in granule cell dendrites is that these dendrites had thresholds greater than the synaptic potential and lower than an action potential. Synaptic activity could not initiate a dendritic spike directly, but an action potential would, once it had been triggered

at a low threshold zone at or near to the soma. The low velocity of invasion (0·1 m/sec) might also be due to poor excitability of the dendrites. Unmyelinated axons of similar or smaller diameter (0·3–1·3 μm) had velocities in the range 0·7–2·3 m/sec (Hodgkin, 1971). Poor excitability of the dendrites could be due to a low concentration of action potential channels, perhaps because of the absence of trophic factors that might operate at the trigger zone or because of spatial competition with post-synaptic receptors (del Castillo & Katz, 1954; Eccles, 1960).

Functional significance of dendritic invasion. The dendritic spikes described here appear to be due to regenerative sodium channels of the type commonly found in axons, and not to the (?)Ca channels described by Llinás & Hess (1976) and Schwartzkroin & Slawsky (1977). They could be present by chance and have no role in the neurones' activity, however, several possibilities exist. For instance, because action potentials usually depolarize membranes more than synaptic activity, the invasion could provide a unique signal to the post-synaptic membrane that the cell had fired. This might be important in resetting the dendritic tree, or in a mechanism for hypothetical modifiable synapses of the type first proposed by Hebb (1949). It has also been suggested that this dendritic invasion could contribute to the accumulation of extracellular K observed in the dendritic layers during repetitive stimulation of the granule cells (Fritz & Gardner-Medwin, 1976).

Hippocampal granule and pyramidal cells often show complex spikes or afterdischarges (Kandel & Spencer, 1961; Ranck, 1975), where a typical unit would fire 2–7 spikes, often decreasing in size, at intervals of 1·5–6·0 msec. Dendritic invasion could cause a depolarization of the soma that outlives its refractory period, and so produce afterdischarges. It is interesting that depolarizing afterpotentials have been recorded from the somata of granule cells (Dudek *et al.* 1976) and of pyramidal cells (Kandel & Spencer, 1961; Schwartzkroin, 1975). The late dendritic sink 3 msec after the soma layer spike in Fig. 1*E* was larger than and close to the site of the earlier synaptic sink. The late sink presumably was prevented from triggering another population spike by residual recurrent inhibition (or refractoriness). The activity of a single granule cell is unlikely to result in appreciable inhibition because of the large convergence of granule onto basket cells, so this mechanism provides a plausible model for the generation of complex spikes.

I wish to thank Dr A. R. Gardner-Medwin for valuable help and criticism during this work, Mr J. V. Halliwell for the loan of histological material, and the M.R.C. for support. Part of this work has been published in abstract form (Jefferys, 1975).

REFERENCES

ANDERSEN, P., BLISS, T. V. P. & SKREDE, K. K. (1971). Unit analysis of hippocampal population spikes. *Expl Brain Res.* **13**, 208–221.

ANDERSEN, P., HOLMQVIST, B. & VOORHOEVE, P. E. (1966). Entorhinal activation of dentate granule cells. *Acta physiol. scand.* **66**, 448–460.

BLISS, T. V. P. & RICHARDS, C. D. (1971). Some experiments with *in vitro* hippocampal slices. *J. Physiol.* **214**, 7–9*P*.

CALVIN, W. H. & HELLERSTEIN, D. (1969). Dendritic spikes vs. cable properties. *Science, N.Y.* **163**, 96–97.

DEADWYLER, S. A., DUDEK, F. E., COTMAN, C. W. & LYNCH, G. (1975). Intracellular responses

of rat dentate gyrus cells *in vitro*: posttetanic potentiation to perforant path stimulation. *Brain Res.* **88**, 80–85.

DEL CASTILLO, J. & KATZ, B. (1954). The membrane change produced by the neuromuscular transmitter. *J. Physiol.* **125**, 546–565.

DUDEK, F. E., DEADWYLER, S. A., COTMAN, C. W. & LYNCH, G. (1976). Intracellular responses of rat hippocampus: perforant path synapse. *J. Neurophysiol.* **39**, 384–393.

ECCLES, J. C. (1960). The properties of dendrites. In *Structure and Function of the Cerebral Cortex*, ed. TOWER, D. B. & SCHADE, J. P., pp. 192–202. Amsterdam: Elsevier.

FATT, P. (1957*a*). Electric potentials occurring around a neurone during its antidromic activation. *J. Neurophysiol.* **20**, 27–60.

FATT, P. (1957*b*). Sequence of events in synaptic activation of a motoneurone. *J. Neurophysiol.* **20**, 61–80.

FRANKENHAEUSER, B. & HODGKIN, A. C. (1957). The action of calcium on the electrical properties of squid axons. *J. Physiol.* **137**, 218–244.

FREEMAN, J. A. & STONE, J. (1969). A technique for current density analysis and its application to the frog cerebellum. In *Neurobiology of Cerebellar Evolution and Development*, ed. LLINÁS, R., pp. 421–430. Chicago: American Medical Association.

FRITZ, L. C. & GARDNER-MEDWIN, A. R. (1976). The effect of synaptic activation on the extracellular potassium concentration in the hippocampal dentate area, in vitro. *Brain Res.* **112**, 183–187.

HEBB, D. O. (1949). *The Organisation of Behaviour*. New York: Wiley.

HODGKIN, A. L. (1971). *The Conduction of the Nervous Impulse*, p. 15. Liverpool: Liverpool University Press.

HUMPHREY, D. (1968). Re-analysis of the antidromic cortical response. I. Potentials evoked by stimulation of the isolated pyramidal tract. *Electroen. clin. Neurophysiol.* **24**, 116–129.

JEFFERYS, J. G. R. (1975). Propagation of action potentials into the dendrites of hippocampal granule cells *in vitro*. *J. Physiol.* **249**, 16–18*P*.

JEFFERYS, J. G. R. (1976). Dendritic spikes in hippocampal cells. *Expl Brain Res.* Suppl. 1, 213–217.

KANDEL, E. R. & SPENCER, W. A. (1961). Electrophysiology of hippocampal neurones. II. Afterpotentials and repetitive firing. *J. Neurophysiol.* **24**, 243–259.

KATZ, B. (1947). The effect of electrolyte deficiency on the rate of conduction in a single nerve fibre. *J. Physiol.* **106**, 411–417.

LLINÁS, R. & HESS, R. (1976). Tetrodotoxin-resistant dendritic spikes in avian Purkinje cells. *Proc. natn. Acad. Sci. U.S.A.* **73**, 2520–2523.

LLINÁS, R. & NICHOLSON, C. (1971). Electrophysiological properties of dendrites and somata in alligator Purkinje cells. *J. Neurophysiol.* **34**, 532–551.

LLINÁS, R., NICHOLSON, C., FREEMAN, J. A. & HILLMAN, D. E. (1968). Dendritic spikes and their inhibition in alligator Purkinje cells. *Science, N.Y.* **160**, 1132–1135.

LØMO, T. (1971). Patterns of activation in a monosynaptic cortical pathway: the perforant path input to the dentate area of the hippocampal formation. *Expl Brain Res.* **12**, 18–45.

NELSON, P. G. & FRANK, K. (1964). Extracellular potential fields of single spinal motoneurones. *J. Neurophysiol.* **27**, 913–927.

NELSON, P. G., FRANK, K. & RALL, W. (1960). Single spinal motoneurone extracellular potential fields. *Fedn Proc.* **19**, 303.

NICHOLSON, C. & FREEMAN, J. A. (1975). Theory of current source-density analysis and determination of conductivity tensor for anuran cerebellum. *J. Neurophysiol.* **38**, 356–368.

NICHOLSON, C. & LLINÁS, R. (1971). Field potentials in the alligator cerebellum and a theory of their relationship to Purkinje cell dendritic spikes. *J. Neurophysiol.* **34**, 509–531.

PAINTAL, A. S. (1973). Conduction in mammalian nerve fibres. In *New Developments in Electromyography and Clinical Neurophysiology*, vol. 2, ed. DESMEDT, J. E., pp. 19–41. Basel: Karger.

RANCK, J. B. (1963). Specific impedance of rabbit cerebral cortex. *Expl Neurol.* **7**, 144–152.

RANCK, J. B. (1975). Behavioral correlates and firing repertoires of neurons in the dorsal hippocampal formation and septum of unrestrained rats. In *The Hippocampus*, vol. 2, ed. ISAACSON, R. L. & PRIBRAM, K. H., pp. 207–246. New York: Plenum.

SCHWARTZKROIN, P. A. (1975). Characteristics of CA1 neurones recorded intracellularly in the hippocampal *in vitro* slice preparation. *Brain Res.* **85**, 423–437.

SCHWARTZKROIN, P. A. & SLAWSKY, M. (1977). Probable calcium spikes in hippocampal neurons. *Brain Res.* **135**, 157–161.

SKREDE, K. K. & WESTGAARD, R. H. (1971). The transverse hippocampal slice: a well-defined cortical structure maintained *in vitro*. *Brain Res.* **35**, 589–593.

SPENCER, W. A. & KANDEL, E. R. (1961). Electrophysiology of hippocampal neurones. IV. Fast prepotentials. *J. Neurophysiol.* **24**, 272–285.

TERZUOLO, C. A. & ARAKI, T. (1961). An analysis of intra- vs. extra-cellular potential changes associated with the activity of single spinal motoneurones. *Ann. N.Y. Acad. Sci.* **94**, 547–558.

YAMAMOTO, C. & KAWAI, N. (1967). Presynaptic action of acetyl choline in thin sections from the guinea pig dentate gyrus *in vitro*. *Expl Neurol.* **19**, 176–187.

YEDLIN, M., KWAN, H., MURPHY, J. T., NGUYEN-HUU, H. & WONG, Y. C. (1974). Electrical conductivity in cat cerebellar cortex. *Expl Neurol.* **43**, 555–569.